RSC Advances

PAPER

View Article Online
View Journal | View Issue

Cite this: *RSC Adv.*, 2021, **11**, 17249

A dynamic evolution model of coal permeability during enhanced coalbed methane recovery by N_2 injection: experimental observations and numerical simulation

Bo Li,[acd] Junxiang Zhang,*[abcd] Zhiben Ding,[a] Bo Wang[a] and Peng Li[b]

China boasts abundant coalbed methane (CBM) resources whose output is significantly influenced by the permeability of coal reservoirs. However, the permeability of coal reservoirs in China is generally low, which seriously restricts the efficient exploitation of CBM. To solve this problem, enhanced coalbed methane (ECBM) recovery by N_2 injection has been widely adopted in recent years. However, there exists little research conducted on coal permeability behavior during the displacement process. In this work, a series of physical simulation experiments were conducted on CH_4 displacement by N_2 injection to investigate the dynamic evolution of coal permeability. Based on the dual-porosity medium property of coal, a dynamic evolution model of coal permeability considering the combined effects of matrix shrinkage/swelling and effective stress was proposed to reflect the ECBM recovery process. The accuracy of this theoretical model was verified by matching the numerical simulation results with the experimental data. The findings show that coal permeability increases at a gradually decelerating rate with the passage of displacement time, and finally tends to be stable. In addition, raising N_2 injection pressure can dramatically enhance CH_4 recovery and shorten the displacement time, which indicates that ECBM recovery by N_2 injection is a feasible technical method for low-permeability coal reservoirs. Meanwhile, the model proposed in this study can be applied to the prediction of CBM production, and is of guiding significance for engineering applications.

Received 2nd April 2021
Accepted 4th May 2021

DOI: 10.1039/d1ra02605d

rsc.li/rsc-advances

1 Introduction

Coalbed methane (CBM) is an unconventional gas sharing a symbiotic relationship with coal. China boasts an abundant CBM reserve whose development and usage are meaningful. According to statistics, over 35 trillion m^3 of CBM are reserved in coal seams less than 2000 m in depth, featuring enormous development potential.[1–3] Since methane (CH_4) is the main component of CBM, the calorific value of 1 m^3 of CBM is up to about 35.9 MJ which is equivalent to that of natural gas. Moreover, CBM is an efficient and clean energy, which does not produce any waste gas after combustion.[4] On the contrary, CBM is also a considerable hazard in underground mining. It may induce gas outbursts and gas explosions that seriously threaten safe production in coal mines. Meanwhile, CBM discharged into the atmosphere may produce a serious greenhouse effect which is 21 times greater than that of CO_2. Such a greenhouse effect is extremely destructive to global ecological environment.[5] Therefore, the exploitation and utilization of the CBM resource is of great significance to both safe mining and environmental protection.

However, the permeability of coal reservoirs in China is generally low, being only 0.01–5 mD, which brings great challenges to underground CBM development.[6,7] Thus, enhancing the permeability of coal reservoirs is the key to improving the efficiency of CBM extraction. Numerous researches have been carried out to investigate the permeability enhancement mechanisms and technologies of coal reservoirs, and measures such as hydraulic flushing, hydraulic fracturing, blasting loosening and advanced borehole have been taken.[8–11] Although these measures achieved a certain effect, but they require a large engineering quantity and can hardly be applied in several mining areas. To resolve this problem, enhanced coalbed methane (ECBM) recovery by gas injection (that is, injecting some gases, such as N_2 or CO_2, into coal seams to displace CBM and promote CBM recovery) has been widely adopted and become a research hotspot worldwide.[12,13] So far, the displacement method has been applied successfully in multiple

[a]*Collaborative Innovation Center of Coal Work Safety and Clean High Efficiency Utilization, Henan Polytechnic University, Jiaozuo, Henan 454003, China. E-mail: zjx@zut.edu.cn; anquanlibo@163.com*

[b]*School of Energy & Environment Engineering, Zhongyuan University of Technology, Zhengzhou, Henan 451191, China*

[c]*State Key Laboratory Cultivation Base for Gas Geology and Gas Control, Henan Polytechnic University, Jiaozuo, Henan 454003, China*

[d]*State and Local Joint Engineering Laboratory for Gas Drainage & Ground Control of Deep Mines, Henan Polytechnic University, Jiaozuo, Henan 454003, China*

countries including American, Australia, India, *etc.*, and achieved fruitful application effects.[14–16] Recently, many scholars have made much research on the displacement mechanism of binary gas flowing in porous media. Based on the molecular motion theory, Hu *et al.*[17] analyzed the self-diffusion and inter-diffusion of CO_2–CH_4 multi component gas systems in coal. Connell *et al.*[18] carried out a series of enhanced drainage core floods to develop a triple porosity model, which realistically described the observed gas migration during the displacement process. Liu *et al.*[19] conducted CO_2-ECBM experiments on cuboid coal samples to monitor the variation on pore pressure, gas flow rate and outlet concentration by increasing injection pressure, also established an effective economic cost model for guiding engineering designs. Kolak and Burruss[20] evaluated the potential of mobilizing non-methane hydrocarbons during CO_2 storage in different rank coal samples, and acquired mobilized amount of polycyclic aromatic hydrocarbons (PAHs) with increasing of coal rank. Ranathunga *et al.*[21] investigated low rank coal samples to analyze the potential for CO_2-ECBM. Result indicated that super-critical CO_2 on CH_4 recovery was independent of coal rank or maturity, whereas high CO_2 pressure may lead to a negative effect on CH_4 production. Zeng *et al.*[22] proposed an internally-consistent adsorption–strain–permeability model, including gas adsorption/desorption, coal deformation, and permeability evolution, and described the ECBM process of CH_4 displacement by CO_2. Moreover, Yang *et al.*[23] conducted molecular simulation to reveal the competitive adsorption mechanism of CH_4, CO_2, and N_2 in coal. Bing *et al.*[24] investigated influences of volumes, frequencies and modes of CO_2 injection on methane production and recovery by numerical simulation.

Previous researches indicate that ECBM recovery by CO_2 injection works as a result of the competitive adsorption between CO_2 and CH_4. Therefore, the adsorption capacity of the coal matrix increases and the coal permeability corresponding decreases, which can not achieve a ideal displacement effect.[25,26] In contrast, ECBM recovery by N_2 injection is more advantageous in low-permeability coal reservoirs. That is due to the adsorption capacity of the coal matrix on N_2 is weaker than that on CH_4, thereby CH_4 cannot be displaced through competitive adsorption.[27] Instead, CH_4 desorption is promoted through reducing the CH_4 partial pressure. Previous studies were mainly focused on the effect of CH_4 displacement, and there is a lack of investigation on the dynamic evolution of coal permeability during CH_4 displacement by N_2 injection.[28] however, lacking related researches on N_2-ECBM to date, the essential mechanism of ECBM recovery by N_2 injection has not been revealed, failing to effectively guide engineering application.

In this study, a series of physical simulation experiments of CH_4 displacement by N_2 injection were performed on the basis of actual coal seam parameters. The combined effects of matrix swelling/shrinkage and effective stress on the dynamic evolution of coal permeability during N_2-ECBM displacement process were analyzed to propose a dynamic evolution model of coal permeability. And the accuracy of the model was verified by matching the numerical simulation results with the experimental data. The findings can serve as a reference for the design, parameter optimization, and theoretical research of gas displacement engineering.

2 Experimental methodology

In the hope of more really reflecting the engineering background, the simulation experiments of CH_4 displacement by N_2 was carried out using large-sized (Φ 100 mm × 300 mm) samples based on the actual coal seam occurrence parameters. And the coal permeability change was detected under different experimental conditions. The coal samples used in the experiments were anthracite collected in Jiulishan Coal Mine, Henan Province, China. Based on BET (low temperature nitrogen adsorption) and industrial analysis methods,[29] the related basic parameters of coal sample are determined. As seen in Table 1, experimental coal samples are rich in pore and fracture structures, which conduces to truly simulating the process of permeation and displacement in original physical state of coal. Therefore, it has a definite guiding significance and reference value for ECBM engineering.

2.1 Experimental system

The experiments of CH_4 displacement by N_2 injection were performed in this work were performed with the self-built displacement system which was mainly composed of a servo loading, gas injection, vacuum extraction, flow measurement, gas sample acquisition, and gas component analysis units. The axial loading on the coal sample was provided by the oil cylinder and stabilized by the accumulator. And the displacement pressure was exerted by the gas cylinder, and the components and concentrations of acquired gas samples during the displacement process were analyzed by the GC-4000A gas chromatograph. The experimental device is illustrated in Fig. 1.

2.2 Preparation of coal samples

Experimental coal samples were anthracite whose initial CBM pressure was 0.5 MPa. First, the raw coal collected from the field was crushed and screened into pulverized coal with the particle size of below 0.25 mm. Then, the screened pulverized coal was evenly added into the displacement chamber and tamped in layers. Finally, the displacement cavity was placed on the experimental platform of the servo machine, and a load of 105 kN was applied on the coal sample at a rate of 100 N s^{-1}, which is equivalent to 13.6 MPa of ground stress, for 24 h to simulate actual occurrence state of coal seam.

2.3 Experimental scheme

2.3.1 Coal permeability tests under different gas source conditions. Firstly, the vacuum unit of the experimental system

Table 1 Related basic parameters of coal sample

Parameter	Value
Total surface area (m^2 g^{-1})	52.8621
Median pore diameter (nm)	8.13
Porosity	0.08
Apparent density (g cm^{-3})	1.49
Water content (%)	4.12
Ash content (%)	9.72
Volatile content (%)	11.18
Fixed carbon	74.98

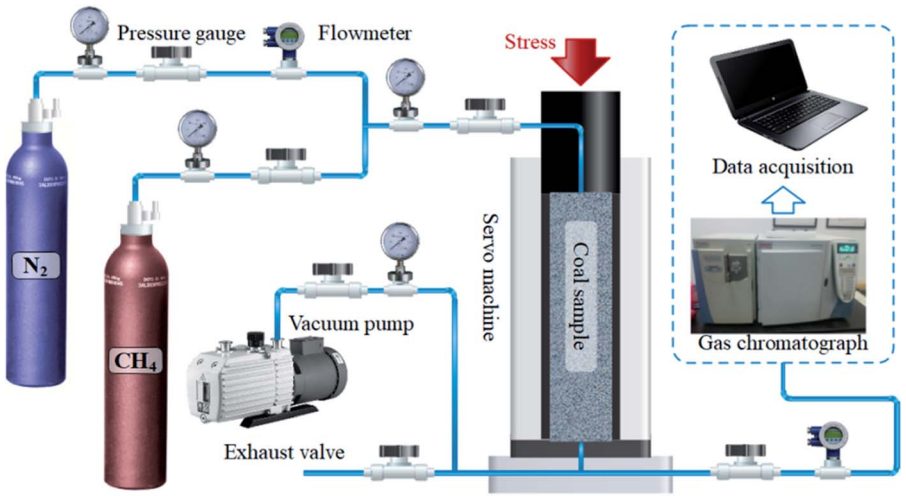

Fig. 1 Diagram of the experimental device.

was turned on to vacuumize the coal samples for more than 12 h, and the pressure in the cavity was less than 100 Pa. Then the coal permeability changes were test by N_2 and CH_4, respectively, under different gas injection pressure. Coal permeability test is carried out by the steady-state method according to Darcy's law, and the permeability calculation formula is expressed as:

$$k = \frac{2Qp_0L\mu}{(p_1^2 - p_2^2)A} \quad (1)$$

where k is coal permeability, m^2; Q is gas flow rate per unit time, $m^3\ s^{-1}$; p_0 is the standard atmospheric pressure, 1.01 × 105 Pa; L is effective seepage length of coal samples, m; μ is dynamic viscosity of the gas, Pa s; p_1 is inlet gas pressure, MPa; p_2 is outlet gas pressure; and A is effective seepage cross-sectional area of coal sample, m^2.

2.3.2 Coal permeability changes during N_2-ECBM process. After the vacuum treatment of the coal samples, the high-purity (99.99%) CH_4 was injected into the cavity until the adsorption pressure of coal samples reached the actual coal seam pressure 0.5 MPa, and the equilibrium time was maintained for more than 24 h. Next, high-purity (99.99%) N_2 was used for simulating ECBM process. Three groups tests were designed in the displacement experiment, with the injection pressure of N_2 was 0.3, 0.5, and 0.7 MPa, respectively. During the process of CH_4 displacement by N_2, the changes of gas flow rates at the inlet and outlet were recorded, and the gases at the outlet were collected regularly.

3 Results and discussion

3.1 Permeability tests of coal to CH_4 and N_2

Permeability test of coal to CH_4 and N_2 has two purposes. One is for analyzing the coal permeability changes under different gas injection pressures, the other is to compare the coal permeability differences between CH_4 and N_2 injection conditions.

As can be seen from the Table 2, under the same gas source condition, coal permeabilities decreases continuously with the rise of gas injection pressure, and the decline rate gradually decelerates. Changing trends of coal permeabilities are displayed in Fig. 2. The fitting results of experimental data indicate that the coal permeabilities shares a negative exponential relationship with the gas injection pressure under different gas injection conditions of CH_4 and N_2, with the squared correlation coefficients R^2 being 0.9312 and 0.9466, respectively. The results are consistent with the permeability test results of Zhao *et al.* on the large size anthracite samples from Qinshui 3# coal seam.[30] It is worth noting that the permeabilities of coal to N_2 is generally higher than that of CH_4 under the same injection pressure. As gas injection pressure is 0.54 MPa, the permeability of coal to N_2 reaches 1.47 times that of CH_4. While the gas injection pressure exceeds a certain threshold, for example, CH_4 pressure is greater than 0.65 MPa, the coal permeability shows a sign of recovery trend with an asymmetric "U" pattern variation.

Due to the dual-porosity medium characteristic of coal, the pore matrix is bound to expand with gas adsorbed in coal. Considering that the surrounding and base of the experimental cavity are rigid, the adsorption swelling of the coal matrix leads

Table 2 Results of coal permeability test

Gas source	Injection pressure (MPa)	Coal permeability (mD)
N_2	0.24	0.78
	0.35	0.62
	0.44	0.44
	0.54	0.37
	0.65	0.30
	0.74	0.27
	0.84	0.26
CH_4	0.25	0.51
	0.35	0.40
	0.48	0.31
	0.54	0.25
	0.64	0.22
	0.76	0.20
	0.8	0.21

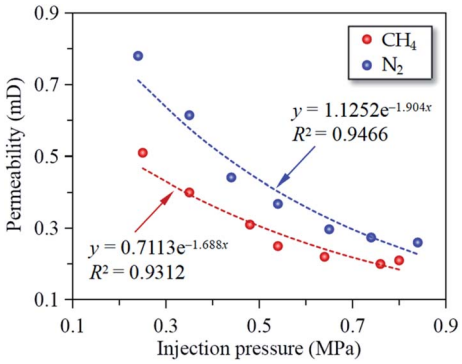

Fig. 2 Coal permeability variation under different gas source and injection pressure conditions.

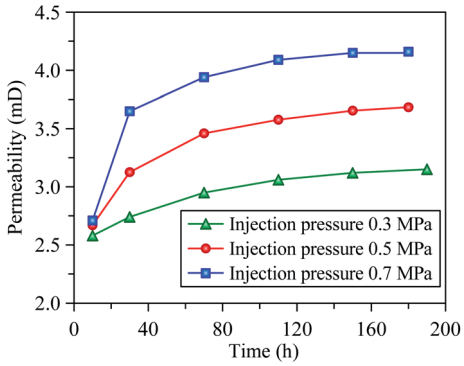

Fig. 3 Coal permeability variation with different N_2 injection pressures.

to shrinkage of the internal seepage channels when a constant stress is applied to the top of the coal sample, which results in a continuous decrease in coal permeability. According to the Langmuir isothermal adsorption curves of coal, the coal adsorption capacity for gas increases with the rise of gas injection pressure, and the adsorption rate gradually decreases and stabilizes until the limit adsorption capacity no longer varies. However, as the pore pressure of coal goes up continuously, the effective stress on the coal sample is reduced. Resultantly, the initially compressed skeleton of the coal matrix expands, which causes the recovery of coal permeability. This phenomenon is also the main reason for the asymmetric U-shaped permeability curve in above-mentioned results. The finding shows that coal permeability change is mainly affected by the adsorption effect of the coal matrix under a low pore pressure. In contrast, the effective stress is dominant at a high pore pressure.

3.2 Coal permeability change during CH_4 displacement by N_2 injection

Above experimental results indicated that coal permeability variations under different gas injection conditions differ to some extent. Therefore, coal permeability is also in a changes dynamically during CH_4 displacement by N_2 injection. In this section, the change of coal permeability during displacement process was analyzed under different injection pressures. The initial gas pressure of the coal sample is 0.5 MPa, and the results are presented in Fig. 3.

As displayed in figure, the variation curves of coal permeability during CH_4 displacement by N_2 injection both present an increasing trend with injection pressure, but the increase rate slows down gradually. Take 0.5 MPa of N_2 gas injection pressure as an example, coal permeability surges rapidly in the initial displacement stage (10–70 min) from the initial 2.67 mD to 3.46 mD by the rate of 0.013 mD min^{-1}. In the middle displacement stage (70–150 min), coal permeability grows slowly from 3.46 mD to 3.66 mD by a reduced rate of 0.003 mD min^{-1}. In the later displacement stage (after 150 min), coal permeability gradually stabilizes at 3.68 mD. The variation curves of coal permeability with different N_2 injection pressures reveal that a high gas injection pressure corresponds to a great increase in coal permeability. Based on the experimental data, as the N_2 injection pressures are 0.3, 0.5, and 0.7 MPa, the coal permeability increases from 2.58, 2.67, and 2.71 mD to 3.15, 3.68, and 4.16 mD, which enhanced by 22.09%, 38.01%, and 53.51%, respectively over the same time span.

The above results indicate that CH_4 displacement by N_2 injection can increase the coal permeability. The reason is due to the coal adsorption capacity of N_2 is weaker than that of CH_4, thereby CH_4 cannot be replaced through competitive adsorption. As a result, CH_4 displacement by N_2 injection causes enhances coal permeability by causing matrix shrinkage. However, the gas adsorption of coal belongs to physical adsorption which is reversible, that is, CH_4 adsorption and desorption can reach to an equilibrium state. Once the CH_4 pressure decreased, the original equilibrium will be broken, then the CH_4 adsorbed on the surface of coal matrix micropores desorb as free gas to reach a new equilibrium, and coal permeability will be changed and finally tended to be stable. Therefore, N_2 injection can achieve the replacement and displacement effect by reducing the effective partial pressure of CH_4 and promotes its desorption.

3.3 Experimental results of CH_4 displacement by N_2 injection

The change curves of N_2 injection, N_2 discharge, and CH_4 discharge volume during CH_4 displacement by N_2 injection are displayed in Fig. 4, which show that CH_4 discharge volume changes in a trend of convex functional form, gradually transitioning from the rapid increase in the initial stage to stable at the late. However, N_2 injection and discharge volume show opposite change trends, which both increase slowly in the initial stage and changed to a linear growth trend later. Comparing with the variation of three curves, we can find that a higher N_2 injection pressure leads to a greater difference between N_2 injection and discharge volume, that is, more residual amount of N_2 is retained in the coal sample. Due to the limited gas adsorption capacity of the coal matrix, the increase in N_2 residual amount results in the decrease of CH_4 partial pressure. Depending on the Langmuir adsorption equation, the

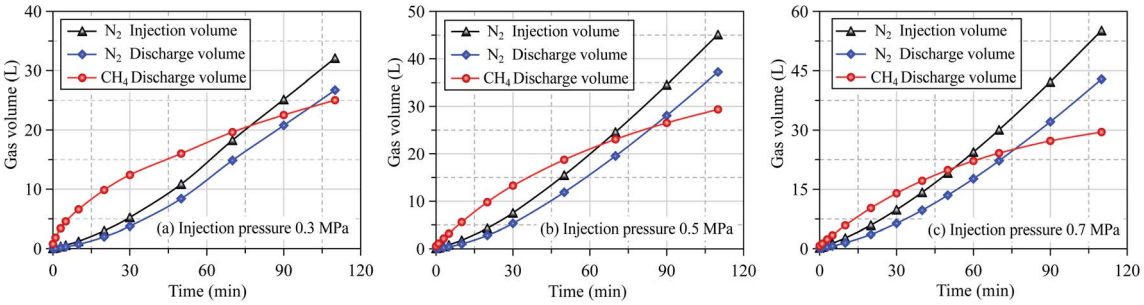

Fig. 4 CH_4 displacement by N_2 injection under different injection pressures.

gas adsorption amount is positively correlated with gas pressure. Therefore, large amounts of adsorbed CH_4 in coal will be desorbed to counter the reduction in CH_4 partial pressure, thus promoting the displacement and production of CH_4. According to the experimental results, the CH_4 adsorption amount of coal sample reaches 36.57 L before N_2 injection. While CH_4 discharge volume corresponding to N_2 injection pressure 0.3, 0.5, and 0.7 MPa at 120 min are 25.04, 29.38, and 29.50 L, with the CH_4 output rate of 68.47%, 80.34% and 80.67%, respectively. Therefore, CH_4 production also increases with N_2 injection pressure at the same displacement time.

Combing with the results of coal permeability change during CH_4 displacement by N_2 injection, it can be found that with N_2 injected into coal, a large amount of N_2 molecules will be absorbed on the surface of the coal matrix. As a result, CH_4 partial pressure falls and coal permeability soars sharply, which leads to CH_4 molecules constantly desorbed from coal matrix and rapidly discharged after N_2 replacement. During this process, the adsorption of N_2 in coal becomes saturated, and coal permeability gradually stabilizes. In this case, the N_2 injection, N_2 discharge, and CH_4 output varies linearly. The experimental results indicate that the coal permeability is a major factor affecting the CH_4 displacement effect. Therefore, the dynamic evolution of coal permeability during displacement should be explored for CBM extraction and production.

4 Dynamic evolution mechanism of coal permeability during CH_4 displacement by N_2 injection

4.1 Dynamic evolution mechanism of coal permeability

The above-mentioned experimental results show that coal permeability changes dynamically during CH_4 displacement by N_2 injection and that the change of coal permeability directly affects the effect of CH_4 discharge and production. As shown in Fig. 5, as a dual-porosity medium, coal comprises micropore-containing matrix and fracture systems. Injection of a certain pressure of N_2 into coal decreases the CH_4 partial pressure and increases the N_2 partial pressure. For this reason, CH_4 molecules desorb constantly from the adsorption state into the free state and spread to the fracture systems, while N_2 molecules shift from the free state into the adsorption state and enter into the pores of the coal matrix. At the macro level, N_2 displaces CH_4 on the pore surface, and then matrix swelling/shrinkage is caused by N_2 adsorption and CH_4 desorption (Fig. 5a and b), thereby affecting the pore volume change of the coal matrix. On the other hand, the injection of N_2 raises the pressure of CH_4 and N_2 gas mixture in the fracture system. According to Terzaghi's effective stress principle, the effective stress of coal will also changed. Relevant researches have disclosed that the coal skeleton deformation induced by the change in effective stress corresponds to the change in the volume of the fracture system, *i.e.*, the deformation of the coal skeleton volume.[31,32] Therefore, the coal permeability during displacement is mainly affected by both matrix swelling/shrinkage and effective stress.

4.2 Effect of matrix swelling/shrinkage and effective stress on coal permeability

4.2.1 Effect of matrix swelling/shrinkage on coal permeability. Previous studies indicated that gas adsorption or desorption occurs in the coal matrix as a result of the change in chemical energy on the pore surface. Once gas adsorption, the free tension of the pore surface will be decreased, thus leading to the decline in the attraction between coal molecules. Thereby, the intermolecular distance enlarged. Macroscopically, this phenomenon is reflected by matrix swelling. In

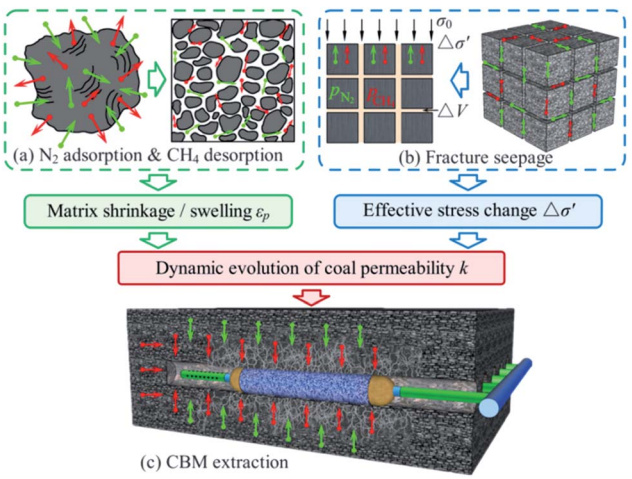

Fig. 5 Evolution mechanism of coal permeability during CH_4 displacement by N_2 injection.

contrast, during gas desorption, the surface chemical energy enhances matrix shrinkage.

Based on the surface chemistry theory,[32] the change in free energy caused by gas adsorption and desorption on the coal surface can be expressed by Gibbs equation:

$$\mathrm{d}(\Delta\pi) = \frac{R_\mathrm{m} T Q \mathrm{d}(\ln p)}{V_\mathrm{m} S} \tag{2}$$

where $\mathrm{d}(\Delta\pi)$ is the change in free energy; R_m is Prussian gas constant, 8.31/(mol K); T is the temperature, K; Q is adsorption amount of gas; S is specific pore surface area; and V_m is mole volume of gas, 22.4 mol L^{-1}.

Since N_2 partial pressure rises from 0 to p_2 and CH_4 partial pressure drops from p_{10} to p_1, the integral of eqn (2) can be obtained as follows:

$$\Delta\pi = \frac{R_\mathrm{m} T}{S V_\mathrm{m}} \left(\int_{p_1}^{p_{10}} \frac{Q_1}{p} \mathrm{d}p - \int_0^{p_2} \frac{Q_2}{p} \mathrm{d}p \right) \tag{3}$$

The adsorption capacity of binary gas in coal conforms to the Langmuir adsorption equilibrium equation:

$$Q_1 = \frac{a_1 b_1 c p_1}{1 + b_1 p_1}, \quad Q_2 = \frac{a_2 b_2 c p_2}{1 + b_2 p_2} \tag{4}$$

where a_1, b_1, a_2 and b_2 are the Langmuir adsorption constants of CH_4 and N_2, respectively, $\mathrm{m}^3\ \mathrm{t}^{-1}$ and Pa^{-1}; c is combustibles mass per unit volume of coal, t m^{-3}; Q_1 and Q_2 are adsorption amount of CH_4 and N_2, respectively.

The variation in free energy on coal surface caused by gas adsorption and desorption can be obtained by simultaneously calculating eqn (2)–(4):

$$\Delta\pi = \frac{R_\mathrm{m} T c}{S V_\mathrm{m}} \left[a_1 \ln\left(\frac{1 + b_1 p_{10}}{1 + b_1 p_1} \right) - a_2 \ln(1 + b_2 p_2) \right] \tag{5}$$

Assuming that coal is under completely ideal constraints, the matrix swelling/shrinkage model of gas adsorption/desorption can be obtained by the principle of elasticity mechanics and energy conservation:[33]

$$\varepsilon_\mathrm{p} = \frac{2\Delta\pi S \rho_\mathrm{v}}{3K} \tag{6}$$

where K is bulk modulus, Pa; and ε_p is volumetric strain of the coal matrix.

By substituting eqn (5) into eqn (6), the following functional relationship between the volumetric strain of the coal matrix and the thermodynamic parameters can be yielded:

$$\varepsilon_\mathrm{p} = \frac{2 c \rho_\mathrm{v} R_\mathrm{m} T}{3 V_\mathrm{m} K} \left[a_1 \ln\left(\frac{1 + b_1 p_{10}}{1 + b_1 p_1} \right) - a_2 \ln(1 + b_2 p_2) \right] \tag{7}$$

Relevant theoretical and experiments verification reveals that over two-thirds of total adsorption swelling strain is the internal swelling strain variable that changes the fracture volume.[34] Assuming that matrix swelling/shrinkage deformation caused during gas adsorption/desorption is reversible. Therefore, during the displacement process, the CH_4 partial pressure falls from p_{10} to p_1, while the N_2 partial pressure rises from 0 to p_2. Then, the volumetric strain of the coal matrix can be expressed as:

$$\varepsilon'_\mathrm{p} = \frac{2}{3}\varepsilon_\mathrm{p} = \frac{4 c \rho_\mathrm{v} R_\mathrm{m} T}{9 V_\mathrm{m} K} \left[a_1 \ln\left(\frac{1 + b_1 p_{10}}{1 + b_1 p_1} \right) - a_2 \ln(1 + b_2 p_2) \right] \tag{8}$$

4.2.2 Effect of effective stress on coal permeability. According to Terzaghi's principle, the difference between the overlying strata stress acting on the coal reservoir and the fluid pressure in pores and fractures is the effective stress, which can be given as:[35]

$$\sigma' = \sigma_0 - \alpha p \tag{9}$$

where σ' is the effective stress of the coal seam, MPa; σ_0 is the overlying strata pressure, MPa; α is Boit's coefficient; and p is the fluid pressure in pores and fractures, MPa.

During the process of CH_4 displacement by N_2 injection, when the CH_4 partial pressure decreases from p_{10} to p_1, the effective stress increases by $\Delta\sigma'_1$. Similarly, when N_2 partial pressure increases from 0 to p_2, the effective stress decreases by $\Delta\sigma'_2$. Therefore, the $\Delta\sigma'$ variation can be obtained as follows:

$$\Delta\sigma' = \alpha(p_{10} - p_1 + p_2) \tag{10}$$

Given that the change in effective stress caused by the change in N_2 and CH_4 gas mixture pressure only induces the volumetric strain of coal skeleton, without altering the swelling/shrinkage amount of coal matrix, thus the coal strain caused by the effective stress variation can be expressed as:[11]

$$\varepsilon_\mathrm{v} = \frac{\Delta\sigma'}{K} = \frac{\alpha(p_{10} - p_1 + p_2)}{K} \tag{11}$$

where ε_v is volumetric strain of the coal.

4.2.3 Dynamic evolution model of coal permeability. Based on the above analysis, the variation in effective stress only changes the volumetric strain of coal skeleton, whereas the matrix swelling/shrinkage alters the volumetric strain of coal matrix. According to the porosity definition,[36] coal porosity equation considering the integrated control of matrix swelling/shrinkage and effective stress can be expressed as follows:

$$\begin{aligned} \varphi &= \frac{V_{p0} - \Delta V_p - \Delta V_t}{V_{t0} - \Delta V_t} = \frac{\left(V_{p0} - \Delta V_p - \Delta V_t\right)/V_{t0}}{\left(V_{t0} - \Delta V_t\right)/V_{t0t}} \\ &= \frac{\varphi_0 + \varepsilon'_\mathrm{p} - \varepsilon_\mathrm{v}}{1 - \varepsilon_v} \end{aligned} \tag{12}$$

Substituting eqn (7) and (10) into (12), we can obtain the porosity evolution model during CH_4 displacement by N_2 injection.

$$\begin{aligned} \varphi = {} & \frac{K\varphi_0 - \alpha(p_{10} - p_1 + p_2)}{K - \alpha(p_{10} - p_1 + p_2)} \\ & + \frac{4 c \rho_\mathrm{v} R_\mathrm{m} T \left[a_1 \ln\left(\frac{1 + b_1 p_{10}}{1 + b_1 p_1} \right) - a_2 \ln(1 + b_2 p_2) \right]}{9 V_\mathrm{m} [K - \alpha(p_{10} - p_1 + p_2)]} \end{aligned} \tag{13}$$

According to the fracture plate model, the model of coal permeability under the combined effects of effective stress and adsorption swelling effect can be expressed by Kozeny–Carman equation.[37]

$$k = k_0\left(\frac{\varphi}{\varphi_0}\right)^3 = k_0\left\{\frac{K\varphi_0 - \alpha(p_{10} - p_1 + p_2)}{\varphi_0[K - \alpha(p_{10} - p_1 + p_2)]} + \frac{4c\rho_v R_m T\left[a_1 \ln\left(\frac{1 + b_1 p_{10}}{1 + b_1 p_1}\right) - a_2 \ln(1 + b_2 p_2)\right]}{\varphi_0 9 V_m[K - \alpha(p_{10} - p_1 + p_2)]}\right\}^3 \quad (14)$$

demonstrates that coal permeability at the initial time (t = 0 min) is equivalent to that of the original state of coal seam unaffected by mining disturbance, with coal permeability is only 2.55 mD.

5 Model validation and discussion

5.1 Establishment of numerical simulation

To verify the correctness of the dynamic evolution model of coal permeability, the numerical simulation by COMSOL Multiphysics software was used to match the results between the simulation outcome and experimental data. For the numerical simulation, the theoretical model was embedded in the PDEs module in the form of partial differential to realize secondary development of the software. And then the physical geometric model of the coal sample with the size of 100 mm × 300 mm was built on the base of actual experimental conditions, as shown in Fig. 6.

The top of the physical model was subjected to uniformly distributed load, the bottom and surrounding boundaries were constrained by vertical or horizontal forces. In the initial state, the adsorption equilibrium pressure of CH_4 gas in the coal sample was 0.5 MPa. The injected N_2 flows through the model from top to bottom, and the displaced CH_4 was discharged from the bottom. The transient solution method was adopted in the numerical calculation.

The main parameters for model calculation are listed in Table 3.

5.2 Analysis of numerical simulation results

Fig. 7 displays the cloud image change of coal permeability during CH_4 displacement by N_2 injection. The graph

While with the passage of displacement time, the coal permeability increases continuously, but the increased extent gradually reduces. Since coal adsorption capacity of N_2 is weaker than that of CH_4, the coal matrix shrinks and the permeability increases after N_2 replaces CH_4. However, as N_2 injection proceeds, the adsorption capacity of the coal matrix becomes saturated. As a result, the strain variation of the coal matrix continuous lowered, thereby coal permeability stabilizes.

Comparison of the simulation results under different N_2 injection pressures can be found that the higher the N_2 injection pressure is, the shorter the time is required for coal permeability to reach the equilibrium state, and the greater increase of permeability is correspondingly. Such a phenomenon demonstrates that raising N_2 injection pressure can significantly enhance the binary gas convection velocity and form a high gas concentration gradient, thus reducing the displacement time. Eqn (10) indicates that a higher N_2 injection pressure corresponds to a smaller effective stress and a larger coal strain, thus leading to a continuously expanding seepage space within coal. Therefore, coal permeability is directly proportional to the gas injection pressure, that is, it increases with the rise of gas injection pressure.

To verify the accuracy of the theoretical model, Fig. 8 presents the matching results between simulation outcome and experimental data of coal permeability during CH_4 displacement by N_2 injection. As can be observed in figure, the both

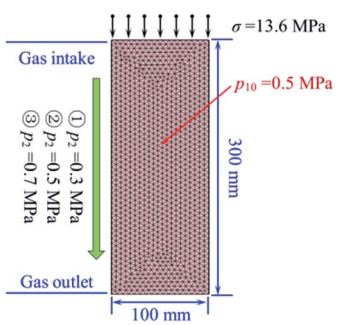

Fig. 6 Physical geometric model.

Table 3 Main parameters for numerical simulation

Parameter	Value
Initial porosity φ_0	0.08
Initial permeability k_0	2.55 mD
CH_4 dynamic viscosity coefficient μ_1	1.03×10^{-5} Pa s
CH_4 Langmuir constant a_1	29.41 kg m^{-3}
CH_4 Langmuir constant b_1	2.25 MPa^{-1}
Coal apparent density ρ_v	1.49 × 103 g m^{-3}
Biot α	0.85
N_2 dynamic viscosity coefficient μ_2	1.69×10^{-5} Pa s
N_2 Langmuir constant a_2	23.15 kg m^{-3}
N_2 Langmuir constant b_2	1.37 MPa^{-1}

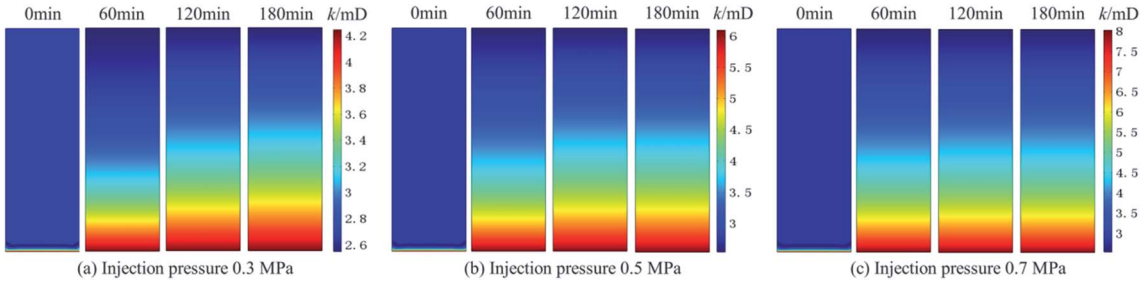

Fig. 7 Cloud image change of coal permeability.

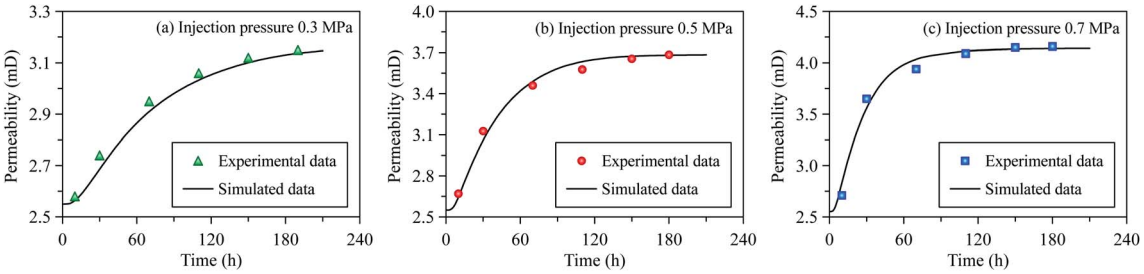

Fig. 8 Matching results between simulation outcome and experimental data.

results share the same change regularity. Coal permeability increases by a gradually decelerating rate with the passage of displacement time and finally stabilizes. The numerical simulation outcome is consistent with the experimental data, thus indicating that the theoretical model can reflect the dynamic evolution of coal permeability during N_2-ECBM process with highly applicable levels.

5.3 Discussion

Experimental results of coal permeability change during displacement process show that N_2 injection can enhance coal permeability and promote CH_4 production and displacement in coal with a positive effect. Therefore, the dynamic evolution model of coal permeability proposed in this work, which comprehensively considers the combined effects of matrix swelling/shrinkage and effective stress, expounds the basic physical process of binary gas relative flow in the process of CH_4 displacement by N_2 injection. Eqn (14) indicates that with the continuous injection of high-pressure N_2 leads to the decrease in CH_4 concentration and the increase in N_2 concentration in fracture space, thereby promoting the rapid diffusion of free CH_4 in the pores and the desorption of adsorbed CH_4 molecule. Compared with the current engineering methods, such as hydraulic fracturing, hydraulic slotting and hydraulic flushing, can significantly improve coal permeability, but the resultant "water-lock" effect may slow down CH_4 diffusion and desorption. In contrast, the method of CH_4 displacement by N_2 injection can avoid the above-mentioned engineering problems and boasts the advantage for enhancing CBM recovery. Based on the theoretical model and COMSOL numerical simulation method proposed in this work, the ECBM effect of N_2 injection and CH_4 discharge volume can be predicted. Therefore, the findings provide an important basis for the design and optimization of displacement engineering and thus serves as a feasible method for ECBM engineering application.

Be noted that, considering the actual influence of geological tectonics and mining activities on coal seam, the large-size raw coal is difficult to collect from the on-site and process into experimental samples as conditions limited. Due to the little discreteness and high repeatability of pulverized coal samples for investigating, this sample is instead of raw coal in this work. Furthermore, related studies also indicate that the permeability response characteristics of both coal samples are basically similar, with little differences in details.[38,39] Besides that, the experimental data of coal permeabilities to CH_4 and N_2 in this work are consistent with researches of Zhao *et al.*,[30] indicating that the pulverized coal samples can be used to investigate the mechanism of N_2-ECBM recovery for providing some guiding significance in engineering application. Therefore, the dynamic evolution model of coal permeability proposed in this work can reflect generally change of coal permeability during CH_4 displacement by N_2 injection. On the basis of the this study, we will conduct relevant field tests in future work to properly modify the theoretical model of eqn (14) for improving the accuracy and applicability to guide actual project.

6 Conclusions

This study carried out a series of physical simulation experiments of CH_4 displacement by N_2 injection under different injection pressure conditions. And a dynamic evolution model of coal permeability considering the combined effects of matrix shrinkage/swelling and effective stress was proposed to reflect

the ECBM recovery process. The main conclusions are obtained as following:

(1) The results of coal permeability tests under different gas source conditions show that coal permeability to N_2 is generally higher than that of CH_4, and the coal permeability changes in an asymmetric "U" pattern trend with the rise of N_2 injection pressure. During CH_4 displacement by N_2 injection, coal permeability continues to increase at a decelerating rate with the passage of displacement time, and finally becomes stable. Increasing N_2 injection pressure is conducive to improving coal permeability and thereby promoting CH_4 production.

(2) Given that coal is a dual-porosity medium, the change in effective stress only changes the volumetric strain of coal skeleton, whereas the coal matrix swelling/shrinkage only alters the volumetric strain of the coal matrix. Based on the porosity equation, a dynamic evolution model of coal permeability considering the combined effects of matrix swelling/shrinkage and effective stress during N_2-ECBM displacement process is established.

(3) The dynamic evolution model of coal permeability was embedded in the PDEs module of COMSOL Multiphysics software in the form of partial differential. Then, theoretical model was calculated by finite element solver to simulation N_2-ECBM effect. And the simulation outcome is consistent with the experimental data, suggesting that the theoretical model can reflect the dynamic evolution of coal permeability during CH_4 displacement by N_2 injection. The findings of this work can provide an important guiding significance for the design and optimization of N_2-ECBM displacement engineering.

Author contributions

All of the authors contributed significantly to this research. Bo Li: conceptualization, investigation, funding. Junxiang Zhang: conceptualization, methodology, investigation, software, writing-original draft. Zhiben Ding: writing-review & editing, supervision, data curation. Bo Wang: visualization, supervision. Peng Li: formal analysis, visualization, software.

Conflicts of interest

There are no conflicts to declare.

Acknowledgements

This work is supported by the National Natural Science Foundation of China (51874125 & 51804356), Research Fund of State and Local Joint Engineering Laboratory for Gas Drainage & Ground Control of Deep Mines (SJF202002), State Key Laboratory Cultivation Base for Gas Geology and Gas Control (WS2020A15), Key Specialized Research and Development Breakthrough in Henan Province (212102310597), Research Funds of Youth Talent and Independent Innovation Research of Zhongyuan University of Technology (K2020QN014 & K2020YY010), Young Key Teachers from Henan Polytechnic University (2019XQG–10), Young Talent Lift Project of Henan Province in 2020 (2020HYTP020), Henan Polytechnic University Foundation for distinguished young (J2020–4).

Notes and references

1 L. H. Xu and C. L. Jiang, Initial desorption characterization of methane and carbon dioxide in coal and its influence on coal and gas outburst risk, *Fuel*, 2017, **203**, 700–706.
2 Y. Z. Chen, J. Li, H. W. Lu and J. Xia, Tradeoffs in water and carbon footprints of shale gas, natural gas, and coal in China, *Fuel*, 2020, **263**, 116778.
3 Y. Qin, A. M. Tim, J. Shen, Z. B. Yang, Y. L. Shen and G. Wang, Resources and geology of coalbed methane in China: A review, *Int. Geol. Rev.*, 2018, **60**, 777–812.
4 P. G. Rutberg, V. A. Kuznetsov, V. E. Popov, S. D. Popov, A. V. Surov, D. I. Subbotin and A. N. Bratsev, Conversion of methane by CO_2 + H_2O + CH_4 plasma, *Appl. Energy*, 2015, **148**, 159–168.
5 J. X. Zhang, B. Li and Y. N. Sun, Dynamic leakage mechanism of gas drainage borehole and engineering application, *Int. J. Min. Sci. Technol.*, 2018, **28**, 505–512.
6 W. Ju, J. Shen, Y. Qin, S. Z. Meng, C. Li, G. Z. Li and G. Yang, *In situ* stress distribution and coalbed methane reservoir permeability in the Linxing area, eastern Ordos Basin, China, *Front. Earth Sci.*, 2018, **12**, 545–554.
7 E. I. Epelle and D. I. Gerogiorgis, A review of technological advances and open challenges for oil and gas drilling systems engineering, *AIChE J.*, 2020, **66**, e16842.
8 N. Li, B. X. Huang, X. Zhang, Y. Y. Tan and B. L. Li, Characteristics of microseismic wave forms induced by hydraulic fracturing in coal seam for coal rock dynamic disasters prevention, *Saf. Sci.*, 2019, **115**, 188–198.
9 J. X. Zhang, B. Li and Y. N. Sun, Performance research of a new coal-dust-based composite sealing material for gas–drainage borehole, *Mater. Express*, 2018, **8**, 325–334.
10 Q. L. Zou, B. Q. Lin, C. S. Zheng, Z. Y. Hao, C. Zhai, T. Liu, J. Y. Liang, F. Z. Yan, W. Yang and C. J. Zhu, Novel integrated techniques of drilling-slotting-separation-sealing for enhanced coal bed methane recovery in underground coal mines, *J. Nat. Gas Sci. Eng.*, 2015, **26**, 960–973.
11 Q. Zou and B. Lin, Fluid–solid coupling characteristics of gas-bearing coal subjected to hydraulic slotting: An experimental investigation, *Energy Fuels*, 2018, **32**, 1047–1060.
12 C. G. Xu, J. Cai and Y. S. Yu, Effect of pressure on methane recovery from natural gas hydrates by methane–carbon dioxide replacement, *Appl. Energy*, 2018, **217**, 527–536.
13 S. S. Tupsakhare and M. J. Castaldi, Efficiency enhancements in methane recovery from natural gas hydrates using injection of CO_2/N_2 gas mixture simulating *in situ* combustion, *Appl. Energy*, 2019, **236**, 825–836.
14 A. Busch and Y. Gensterblum, CBM and CO_2-ECBM related sorption processes in coal: a review, *Int. J. Coal Geol.*, 2011, **87**, 49–71.
15 S. J. Zheng, Y. B. Yao, D. Elsworth, D. M. Liu and Y. D. Cai, Dynamic fluid interactions during CO_2-ECBM and CO_2

sequestration in coal seams. Part I: CO_2–CH_4 interactions, *Energy Fuels*, 2020, **34**, 8274–8282.

16 S. K. Sinha and S. D. Gupta, A geological model for enhanced coal bed methane (ECBM) recovery process: a case study from the Jharia coalfield region, India, *J. Pet. Sci. Eng.*, 2021, **201**, 108498.

17 H. X. Hu, L. Du, Y. F. Xing and X. C. Li, Detailed study on self- and multicomponent diffusion of CO_2–CH_4, gas mixture in coal by molecular simulation, *Fuel*, 2017, **187**, 220–228.

18 L. D. Connell, R. Sander, Z. Pan, M. Camilleri and D. Heryanto, History matching of enhanced coal bed methane laboratory core flood tests, *Int. J. Coal Geol.*, 2011, **87**, 128–138.

19 Z. D. Liu, Y. P. Cheng, Y. K. Wang, L. Wang and W. Li, Experimental investigation of CO_2 injection into coal seam reservoir at in–situ stress conditions for enhanced coalbed methane recovery, *Fuel*, 2019, **236**, 709–716.

20 J. J. Kolak and R. C. Burruss, Geochemical investigation of the potential for mobilizing non-methane hydrocarbons during carbon dioxide storage in deep coal beds, *Energy Fuels*, 2006, **20**, 566–574.

21 A. S. Ranathunga, M. S. A. Perera, P. G. Ranjith and C. H. Wei, An experimental investigation of applicability of CO_2 enhanced coal bed methane recovery to low rank coal, *Fuel*, 2017, **189**, 391–399.

22 Q. S. Zeng, Z. M. Wang, L. Q. Liu and J. P. Ye, Modeling CH_4 displacement by CO_2 in deformed coalbeds during enhanced coalbed methane recovery, *Energy Fuels*, 2018, **32**, 1942–1955.

23 Z. Z. Yang, S. Yang, J. X. Han and X. G. Li, Molecular simulation on competitive adsorptions of CO_2, CH_4, and N_2 in deep coal seams, *Chem. Technol. Fuels Oils*, 2020, **56**, 619–626.

24 Z. Bing, J. P. Ye, Y. Li, X. T. Han, J. Shen and C. Cao, Simulation of key parameters in CO_2 injection for enhanced coalbed methane recovery in a deep well group, *Energy Sources, Part A*, 2018, **40**, 2219–2226.

25 C. J. Fan, D. Elsworth, S. Li, Z. W. Chen, M. K. Luo, Y. Song and H. H. Zhang, Modelling and optimization of enhanced coalbed methane recovery using CO_2/N_2 mixtures, *Fuel*, 2019, **253**, 1114–1129.

26 S. A. Mathias, S. Nielsen and R. L. Ward, Storage coefficients and permeability functions for coal-bed methane production under uniaxial strain conditions, *Transp. Porous Media*, 2019, **130**, 627–636.

27 Y. Li, Z. Yang and X. G. Li, Molecular simulation study on the effect of coal rank and moisture on CO_2/CH_4 competitive adsorption, *Energy Fuels*, 2019, **33**, 9087–9098.

28 X. D. Du, M. Gu, Z. J. Liu and Y. Zhao, Enhanced shale gas recovery by the injections of CO_2, N_2 and CO_2/N_2 mixture gases, *Energy Fuels*, 2019, **33**, 5091–5101.

29 K. H. Shi, E. E. Santiso and K. E. Gubbins, Bottom-up approach to the coarse-grained surface model: Effective solid–fluid potentials for adsorption on heterogeneous surfaces, *Langmuir*, 2019, **35**(17), 5975–5986.

30 Y. S. Zhao, Y. Q. Hu, D. Yang and J. P. Wei, Experimental study of the gas seepage law of rock related to adsorption under 3D stresses, *Chin. J. Rock Mech. Eng.*, 1999, **18**, 651–653.

31 J. P. Wei, B. Li, K. Wang and D. H. Sun, 3D numerical simulation of boreholes for gas drainage based on the pore-fracture dual media, *Int. J. Min. Sci. Technol.*, 2016, **26**, 739–744.

32 C. Liu and Y. G. Zhang, Interpretation of Gibbs surface excess model for gas adsorption on heterogeneous coal particle, *Fuel*, 2018, **214**, 20–25.

33 P. Guo, S. G. Cao, Z. G. Zhang, F. Luo and Y. B. Liu, Theoretical study of deformation model of coal swelling induced by gas adsorption, *Rock Soil Mech.*, 2014, **35**, 128–133.

34 J. P. Zhou, X. F. Xian and Y. D. Jiang, A model of adsorption induced coal deformation based on thermodynamics approach, *J. China Coal Soc.*, 2011, **36**, 468–472.

35 A. Gilman and R. Beckie, Flow of coal-bed methane to a gallery, *Transp. Porous Media*, 2000, **41**, 1–16.

36 Z. Sun, J. T. Shi, T. Zhang, K. L. Wu, D. Feng, F. R. Sun, L. Huang, C. H. Hou and X. F. Li, A fully-coupled semi–analytical model for effective gas/water phase permeability during coal-bed methane production, *Fuel*, 2018, **223**, 44–52.

37 J. X. Zhang, Y. W. Liu, P. L. Ren, H. K. Han and S. Zhang, A fully multifield coupling model of gas extraction and air leakage for in-seam borehole, *Energy Rep.*, 2021, **7**, 1293–1305.

38 S. G. Li, Y. Li, P. Guo, Y. J. Yan and Y. B. Liu, Comparative research on permeability characteristics in complete stress–strain process of briquettes and coal samples, *Chin. J. Rock Mech. Eng.*, 2010, **29**, 899–906.

39 H. Y. Jia, K. Wang, Y. B. Wang and K. X. Sun, Permeability characteristics of gas-bearing coal specimens under cyclic loading–unloading of confining pressure, *J. China Coal Soc.*, 2020, **45**, 1710–1718.